

Charge diffusion in the one-dimensional Hubbard model

R. Steinigeweg,^{1,*} F. Jin,² H. De Raedt,³ K. Michielsen,^{2,4} and J. Gemmer^{1,†}

¹*Department of Physics, University of Osnabrück, D-49069 Osnabrück, Germany*

²*Institute for Advanced Simulation, Jülich Supercomputing Centre, Forschungszentrum Jülich, D-52425 Jülich, Germany*

³*Zernike Institute for Advanced Materials, University of Groningen, NL-9747AG Groningen, The Netherlands*

⁴*RWTH Aachen University, D-52056 Aachen, Germany*

(Received 16 February 2017; published 28 August 2017)

We study the real-time and real-space dynamics of charge in the one-dimensional Hubbard model in the limit of high temperatures. To this end, we prepare pure initial states with sharply peaked density profiles and calculate the time evolution of these nonequilibrium states, by using numerical forward-propagation approaches to chains as long as 20 sites. For a class of typical states, we find excellent agreement with linear-response theory and unveil the existence of remarkably clean charge diffusion in the regime of strong particle-particle interactions. We additionally demonstrate that, in the half-filling sector, this diffusive behavior does not depend on certain details of our initial conditions, i.e., it occurs for five different realizations with random and nonrandom internal degrees of freedom, single and double occupation of the central site, and displacement of spin-up and spin-down particles.

DOI: [10.1103/PhysRevE.96.020105](https://doi.org/10.1103/PhysRevE.96.020105)

Introduction. Static properties of integrable quantum many-body systems are well understood [1]. In contrast, dynamical questions in these systems continue to be a major challenge in many areas of modern physics and range from fundamental questions in statistical physics to applied questions for a specific class of materials. On the one hand, integrable systems feature a macroscopic number of (quasi)local conservation laws [2–4] and any overlap with these conserved quantities leads to the breakdown of conventional equilibration and thermalization [5,6]. On the other hand, such an overlap is not warranted for all possible initial states, observables, or model parameters, and integrability does not rigorously exclude the existence of thermodynamic relaxation such as exponential decay or diffusive transport. This type of relaxation, however, is often traced back to chaos [7,8], being absent in integrable systems.

In this context, two important and extensively studied examples are (i) the one-dimensional XXZ spin- $\frac{1}{2}$ model and (ii) the (Fermi-)Hubbard chain. As typical for integrable systems, the energy current is (i) strictly or (ii) at least partially conserved [2] such that energy flow is ballistic at any finite temperature [9–12], as signaled by a nonzero Drude weight within linear-response theory. However, a much richer dynamical phase diagram develops for other transport quantities. In case (i) of the XXZ spin- $\frac{1}{2}$ chain, the spin current is not strictly conserved. While the partial conservation of this current and a nonzero Drude have been proven analytically below the isotropic point [3,4,13,14], strong numerical evidence for a vanishing Drude weight and nonballistic dynamics has been provided above this point [15–19]. In fact, for the latter regime, clear signatures of diffusion have been reported in various works [11,20–22]. In case (ii) of the Hubbard chain, the situation appears to be similar for charge transport. Even though clarifying the existence of a nonzero Drude weight has turned out to be hard task analytically [23–26], numerical

studies point to a vanishing Drude weight for strong particle-particle interactions [27–29]. While signatures of diffusion have been observed for such interactions also [29–32], a direct detection of the characteristic Gaussian broadening is lacking.

The intention of our Rapid Communication is to clarify the existence of charge diffusion in the Hubbard chain. For this purpose, we study the nonequilibrium dynamics as resulting for a convenient class of initial states. These initial states are pure and realize density profiles where a peak with a maximum possible amplitude is located in the center of the chain and lies on top of a homogeneous many-body background. First, we focus on a subclass with random internal degrees of freedom and rely on the well-known concept of typicality [33–46] to obtain the real-time broadening of density profiles in the linear-response regime. In this regime, our large-scale numerical simulations for chains as long as 20 sites allow us to unveil the existence of remarkably clean charge diffusion, as a key result of our Rapid Communication. Finally, we extend our analysis to initial states without any randomness and show that the dynamical behavior is stable against varying details of the initial conditions. This stability is another central result of our work and reveals that exactly the same charge diffusion emerges in a far-from-equilibrium setup. These findings clearly demonstrate that thermodynamic relaxation can occur in integrable systems.

Model and observables. In one spatial dimension and with periodic boundary conditions, the Hamiltonian of the Hubbard model reads $H = \sum_{r=1}^L h_r$,

$$h_r = -t_h \sum_{s=\downarrow,\uparrow} (a_{r,s}^\dagger a_{r+1,s} + \text{H.c.}) + U \left(n_{r,\downarrow} - \frac{1}{2} \right) \left(n_{r,\uparrow} - \frac{1}{2} \right), \quad (1)$$

where the operator $a_{r,s}^\dagger$ ($a_{r,s}$) creates (annihilates) at site r a fermion with spin s , t_h is the hopping matrix element, and L is the number of sites. The operator $n_{r,s} = a_{r,s}^\dagger a_{r,s}$ is the local occupation number and U is the strength of the

*rsteinig@uos.de

†jgemmer@uos.de

on-site interaction. For all values, this model is integrable and the total particle numbers $N_s = \sum_r n_{r,s}$ and $N = N_\downarrow + N_\uparrow$ are strictly conserved quantities. We do not restrict ourselves to a particular particle sector, i.e., we study the case $\langle N \rangle = L$ [47]. It is worth mentioning that, via the Jordan-Wigner transformation, this model can be mapped onto a spin- $\frac{1}{2}$ two-leg ladder of length L , with XY exchange in the legs and Ising exchange in the rungs [31]. In fact, this spin model is used in our numerical simulations.

We are interested in the real-time dynamics of the local occupation numbers $n_{r,s}$ and investigate the expectation values $p_{r,s}(t) = \text{tr}[n_{r,s} \rho(t)]$ for the density matrix $\rho(t)$ at time t . (It is important to note that t and t_h are different parameters.) Doing so, we can follow the broadening of nonequilibrium density profiles, as realized by the preparation of a proper initial state $\rho(0)$.

Initial states. In this Rapid Communication, we prepare pure initial states $\rho(0) = |\psi(0)\rangle\langle\psi(0)|$. To specify our $|\psi(0)\rangle$, it is convenient to consider the common eigenbasis of all $n_{r,s}$. Let $|\phi_k\rangle$ be this basis. Then, our initial states read

$$|\psi(0)\rangle \propto n_{L/2,\uparrow}|\phi\rangle, \quad |\phi\rangle = \sum_{k=1}^{4^L} c_k |\phi_k\rangle, \quad (2)$$

where c_k are complex and yet arbitrary coefficients. Since $n_{L/2,\uparrow}$ projects only onto states with a spin-up particle in the middle of the chain, $p_{L/2,\uparrow}(0) = 1$ has the maximum value possible.

Here, we focus on two particular choices for the coefficients c_k . First, we choose all c_k to be the same number. Second, we choose the c_k at random according to the unitary invariant Haar measure [37]. This choice means in practice that the real and imaginary parts of the c_k are independently drawn from a Gaussian distribution with zero mean. For both the random and equal choice of the c_k , all $p_{r \neq L/2, s \neq \uparrow}(0) = p_{\text{eq}} = \frac{1}{2}$ take on their equilibrium value, and still $p_{L/2,\uparrow}(0) = 1$. Therefore, the initial density profile features a central peak on top of a homogeneous many-particle background.

A very similar form for the density profile also results for the state

$$|\psi_{\text{double}}(0)\rangle \propto n_{L/2,\downarrow}|\psi(0)\rangle. \quad (3)$$

Then, due to the additional projection, $p_{L/2,\downarrow}(0) = 1$ also for equal and random c_k . Therefore, the density profiles $p_{r,\uparrow}(t) = p_{r,\downarrow}(t)$ are identical for $t = 0$ and all later times $t > 0$ as well (see Ref. [47] for the initial displacement).

All initial states introduced have to be considered as far-from-equilibrium states: They are not only pure but also have maximum $p_{L/2,\uparrow}(0) = 1$. Remarkably, however, the dynamics of $|\psi(0)\rangle$ in Eq. (2) with random c_k can be connected to the linear-response Kubo formula, since the underlying $|\phi\rangle$ is a so-called typical state [22] (see also Refs. [33–46] for the concept of typicality). Exploiting this typicality allows one to derive the relation [47]

$$p_{r,\uparrow}(t) - p_{\text{eq}} = 2\langle (n_{L/2,\uparrow} - p_{\text{eq}})(n_{r,\uparrow}(t) - p_{\text{eq}}) \rangle, \quad (4)$$

where $\langle \cdot \rangle = \text{tr}[\cdot]/4^L$ is the thermodynamic average at formally infinite temperatures. Thus, for a typical state, the nonequilibrium expectation value is directly related to an equilibrium correlation function. This fact enables a connection to the

Kubo formula via the variance

$$\sigma(t)^2 = \sum_{r=1}^L r^2 \delta p_{r,\uparrow}(t) - \left[\sum_{r=1}^L r \delta p_{r,\uparrow}(t) \right]^2, \quad (5)$$

where $\delta p_{r,\uparrow}(t) = 2[p_{r,\uparrow}(t) - p_{\text{eq}}]$ excludes the equilibrium background and is normalized to $\sum_r \delta p_{r,\uparrow}(t) = 1$. As shown in Ref. [48], the time derivative of this variance satisfies

$$\frac{d}{dt} \sigma(t)^2 = 2D(t), \quad D(t) = \frac{4}{L} \int_0^t dt' \langle j_\uparrow(t') j_\uparrow \rangle, \quad (6)$$

where $j_\uparrow = -t_h \sum_r (i a_{r,\uparrow}^\dagger a_{r+1,\uparrow} + \text{H.c.})$ is the total current of the spin-up particles and the quantity $D(t)$ plays the role of a time-dependent diffusion coefficient. For $U = 0$, $[j_\uparrow, H] = 0$ necessarily leads to ballistic scaling $D(t) \propto t$ and $\sigma(t) \propto t$. For large $U \gg t_h$, signatures of diffusive scaling $D(t) = \text{const}$ and $\sigma(t) \propto \sqrt{t}$ have been reported in Refs. [29,30]. So far, however, a systematic analysis beyond the mere width of the density profile is lacking and is the central issue of our work.

Numerical technique and results. From a numerical point of view, the Hubbard chain is challenging since the Hilbert-space dimension $\text{dim} = 4^L$ grows rapidly with L , e.g., much faster than the also exponential increase $\text{dim} = 2^L$ in case of a spin- $\frac{1}{2}$ chain. As a consequence, exact diagonalization of the Hamiltonian is only feasible for a few lattice sites and a real-space experiment such as the one done in our Rapid Communication would not be reasonable. Hence, we proceed differently and profit from the fact that we only need to deal with pure states. The time evolution of these states can be obtained by forward-propagation methods such as fourth-order Runge-Kutta [18,19,41] or more sophisticated schemes such as Trotter decompositions or Chebyshev polynomials [29,49,50]. We apply a second-order Trotter formula with a time step $\delta t t_h = 0.05$, sufficient to reach very good agreement with

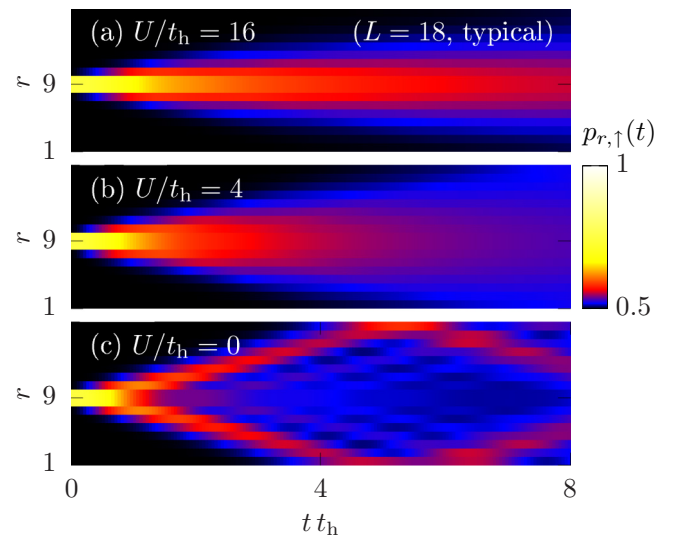


FIG. 1. Time-space density plot of the spin-up occupation numbers $p_{r,\uparrow}(t)$ for a typical initial state $|\psi(0)\rangle$ [where all spin-down occupation numbers $p_{r,\downarrow}(0) = p_{\text{eq}}$] in the one-dimensional Hubbard model with $L = 18$ sites and different interaction strengths: (a) $U/t_h = 16$, (b) $U/t_h = 4$, (c) $U/t_h = 0$. While the broadening in (a) points to charge diffusion, the broadening in (c) is clearly ballistic.

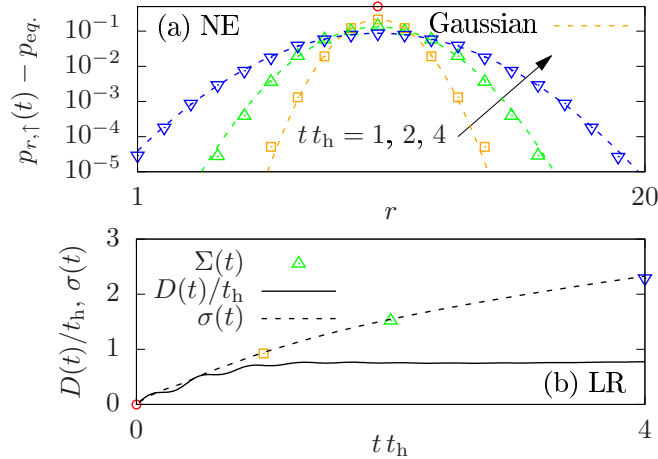


FIG. 2. (a) Density profile $p_{r,\uparrow}(t)$ as a function of site r at various times $t t_h = 0, 1, 2, 4$ for a Hubbard chain of length $L = 20$ and with a strong interaction $U/t_h = 16$, shown in a semilog plot (symbols). [The initial state $|\psi(0)\rangle$ is the same as the one in Fig. 1.] The data can be described by Gaussian fits over several orders of magnitude (curves). (b) Linear-response result for the time evolution of the diffusion coefficient $D(t)$ and profile width $\sigma(t)$, as obtained in Ref. [29] for length $L = 18$ and the same interaction $U/t_h = 16$ (curves). The standard deviation $\Sigma(t)$, as resulting from the Gaussian fits in (a), is indicated for comparison (symbols).

Chebyshev-polynomial algorithms. A massively parallelized implementation of this formula allows us to treat Hubbard chains as long as $L = 20$ sites. For this system size and a maximum time $t t_h = 8$, the simulation takes about 9 h when using 262 144 double-thread cores. Therefore, apart from the $L = 20$ data depicted in Fig. 2, we focus on $L = 18$ to reduce computational costs at least a bit.

Now, we turn to our numerical results. We start with the initial state $|\psi(0)\rangle$ in Eq. (2) with a random choice of the coefficients c_k , i.e., a typical state. It is important to note that we consider a single realization of the c_k and do not perform any kind of averaging. Still, we allow the c_k to be different for each simulation. In Figs. 1(a)–1(c) we depict our results for the spin-up occupation numbers $p_{r,\uparrow}(t)$ for a Hubbard chain of length $L = 18$ and with different interactions $U/t_h = 16, 4, 0$, in a two-dimensional (2D) time-space density plot. Several comments are in order. First, for the noninteracting case $U = 0$ in Fig. 1(c), the real-time broadening of $p_{r,\uparrow}(t)$ is clearly linear and, as discussed above, has to occur due to the strict conservation of the particle current. The pronounced jets visible are typical for free-particle cases [11,22] and propagate fast without any scattering until they eventually hit the boundary of the chain at short times $t t_h \sim 4$. Second, for the interacting cases $U/t_h = 16$ and 4 in Figs. 1(a) and 1(b), these jets and the linear broadening disappear as well, i.e., the dynamics is not ballistic. Note that, in contrast, the flow of energy is ballistic for arbitrary U [47]. Third, the broadening is the slower the larger U because scattering becomes stronger as U increases. In particular, for the largest $U/t_h = 16$ in Fig. 1(a) and the maximum time $t t_h = 8$ calculated, the overall width of $p_{r,\uparrow}(t)$ is still smaller than the chain length. Therefore, we can exclude trivial finite-size effects for such times [47].

To gain insight into the dynamics at large $U/t_h = 16$, we show in Fig. 2(a) the site dependence of the profile $p_{r,\uparrow}(t)$ for various times $t t_h = 0, 1, 2, 4$, and for an even larger system size $L = 20$. We do so by subtracting from $p_{r,\uparrow}(t)$ the equilibrium value p_{eq} and using a semilog plot, to visualize also the outer tails of the profile. It is intriguing to see that, for all times t depicted, the profiles can be described very well by Gaussians,

$$p_r(t) - p_{eq} = \frac{1}{2} \frac{1}{\sqrt{2\pi} \Sigma(t)} \exp \left[-\frac{(r - L/2)^2}{2 \Sigma(t)^2} \right], \quad (7)$$

where the standard deviation $\Sigma(t)$ occurs as the only free parameter and is adjusted by fitting. The excellent fits over several orders of magnitude are a central result of our work and already provide strong evidence for the existence of diffusion. Still, however, $\Sigma(t)$ needs to scale as $\Sigma(t) \propto \sqrt{t}$.

For a final conclusion, we show in Fig. 2(b) the time dependence of $\Sigma(t)$ and compare to the linear response $\sigma(t)$ in Eq. (6), as resulting from the $D(t)$ calculated in Ref. [29] for the same interaction $U/t_h = 16$ and length $L = 18$. While the perfect agreement illustrates the high accuracy of the typicality relation, this agreement implies that the linear-response result $D(t) = \text{const}$ [29,30] also holds for our nonequilibrium dynamics. Thus, diffusion clearly exists. Note that the same conclusion can be drawn for smaller interactions $U/t_h = 8$ also [47], where finite-size effects are still negligibly small. For $U/t_h \ll 8$, however, significant finite-size effects are known to occur [29] and a reliable conclusion on the thermodynamic limit $L \rightarrow \infty$ is impossible on the basis of $L \sim 20$.

Next, we intend to shed light on the role of the specific initial-state realization, in particular, on the influence of randomness. Therefore, in a first step, we investigate the initial state $|\psi(0)\rangle$ in Eq. (2) again but now with equal coefficients c_k . Recall that, while this nonrandom state has exactly the same

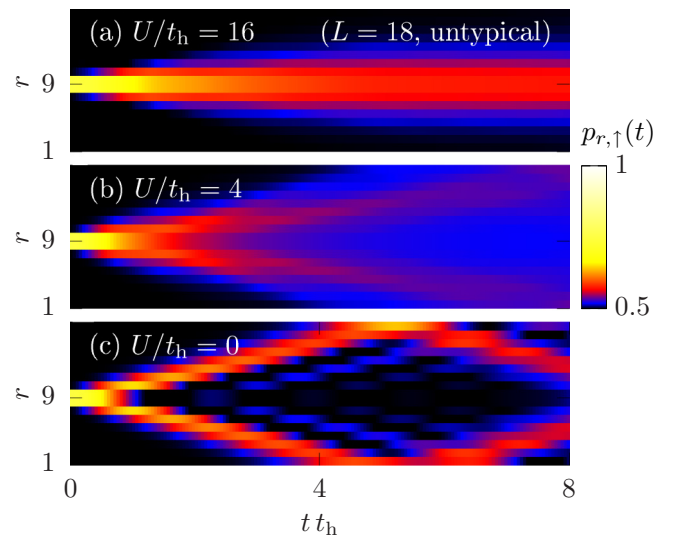


FIG. 3. Time-space density plot of the spin-up occupation numbers $p_{r,\uparrow}(t)$ for the same model parameters as in Fig. 1 but for another and *untypical* initial state $|\psi(0)\rangle$ [where all spin-down occupation numbers $p_{r,\downarrow}(0) = p_{eq}$ once again]. Compared to Fig. 1, jetlike behavior is enhanced in (c) while no significant difference is visible in (a).

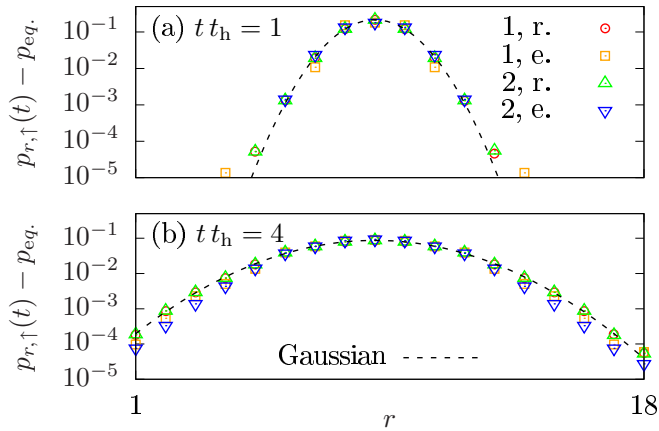


FIG. 4. Density profile $p_{r,\uparrow}(t)$ vs site r for fixed times (a) $t t_h = 1$, (b) $t t_h = 4$ for various initial states, i.e., $|\psi(0)\rangle$ (1) and $|\psi_{\text{double}}(0)\rangle$ (2) with random (r.) and equal (e.) coefficients in the underlying superposition. As a guide to the eyes, Gaussian fits are indicated (for 1, r.). While data for random initial states are practically indistinguishable, data for nonrandom initial states differ only very little.

initial density profile, the typicality relation does not need to hold any further. For this state, we repeat the calculation in Fig. 1 for $L = 18$ sites and different interactions $U/t_h = 16, 4, 0$ and summarize the corresponding results in Fig. 3. In comparison to Fig. 1, jetlike behavior for $U = 0$ is enhanced in Fig. 3(c) and emerges now for $U/t_h = 4$ in Fig. 3(b) in addition. The same observation has been made for the XXZ spin- $\frac{1}{2}$ chain below the isotropic point [22]. Remarkably, however, the diffusive behavior for $U/t_h = 16$ in Fig. 3(a) turns out to be unaltered. In fact, this observation is different to the one found for the XXZ spin- $\frac{1}{2}$ chain above the isotropic point [22], where the impact of nonrandomness is strong.

The above finding suggests that charge diffusion for strong interactions U is stable against varying details of the initial condition. To substantiate this suggestion, we finally extend

our analysis to the initial state $|\psi_{\text{double}}(0)\rangle$ in Eq. (3) and study both random and equal coefficients c_k . To repeat, these states have the same initial density profile $p_{r,\uparrow}(0)$ but $p_{r,\downarrow}(0) = p_{r,\uparrow}(0)$ now. For system size $L = 18$, interaction $U/t_h = 16$, and two different times $t t_h = 1, 4$, we compare in Fig. 4 the distribution $p_{r,\uparrow}(t)$ for these states with the one for the others. Apparently, $p_{r,\uparrow}(t)$ is practically indistinguishable for the two cases with random c_k . Even though not shown explicitly here, these two random cases also coincide for other values of U [47]. While the two equal cases in Fig. 4 differ from the two random ones, this difference is minor in view of the semilog plot used. These observations are another central result of our work and clearly show that charge diffusion in the strong-interaction limit does not depend on the specific initial-state preparation, at least for the whole class of nonequilibrium states investigated and at half filling.

Conclusions. In this Rapid Communication, we have investigated the real-time broadening of charge in the Hubbard chain at high temperatures. First, we have introduced a class of pure initial states with density profiles where a sharp peak is located in the middle of the chain and lies on top of a homogeneous many-particle background. Then, we have calculated the dynamics of these nonequilibrium states, by using large-scale numerical simulations. Our results for typical states have unveiled the existence of remarkably clean charge diffusion in the limit of strong particle-particle interactions, in perfect agreement with the Kubo formula. We have additionally demonstrated that, in the half-filling sector, this diffusive behavior is stable against varying details of the initial conditions and occurs for nonrandom states as well. Promising future directions of research include the extension of our work to lower temperatures and other fillings.

Acknowledgments. We sincerely thank T. Prosen and F. Heidrich-Meisner for fruitful discussions. In addition, we gratefully acknowledge the computing time, granted by the “JARA-HPC Vergabegremium” and provided on the “JARA-HPC Partition” part of the supercomputer “JUQUEEN” [51] at Forschungszentrum Jülich.

-
- [1] D. C. Johnston, R. K. Kremer, M. Troyer, X. Wang, A. Klümper, S. L. Bud’ko, A. F. Panchula, and P. C. Canfield, *Phys. Rev. B* **61**, 9558 (2000).
- [2] X. Zotos, F. Naef, and P. Prelovšek, *Phys. Rev. B* **55**, 11029 (1997).
- [3] T. Prosen, *Phys. Rev. Lett.* **106**, 217206 (2011).
- [4] T. Prosen and E. Ilievski, *Phys. Rev. Lett.* **111**, 057203 (2013).
- [5] M. Rigol, V. Dunjko, V. Yurovsky, and M. Olshanii, *Phys. Rev. Lett.* **98**, 050405 (2007).
- [6] E. Ilievski, J. De Nardis, B. Wouters, J.-S. Caux, F. H. L. Essler, and T. Prosen, *Phys. Rev. Lett.* **115**, 157201 (2015).
- [7] C. Mejía-Monasterio, T. Prosen, and G. Casati, *Europhys. Lett.* **72**, 520 (2005).
- [8] L. D’Alessio, Y. Kafri, A. Polkovnikov, and M. Rigol, *Adv. Phys.* **65**, 239 (2016).
- [9] A. Klümper and K. Sakai, *J. Phys. A: Math. Gen.* **35**, 2173 (2002).
- [10] S. Langer, M. Heyl, I. P. McCulloch, and F. Heidrich-Meisner, *Phys. Rev. B* **84**, 205115 (2011).
- [11] C. Karrasch, J. E. Moore, and F. Heidrich-Meisner, *Phys. Rev. B* **89**, 075139 (2014).
- [12] C. Karrasch, D. M. Kennes, and F. Heidrich-Meisner, *Phys. Rev. Lett.* **117**, 116401 (2016).
- [13] X. Zotos, *Phys. Rev. Lett.* **82**, 1764 (1999).
- [14] J. Benz, T. Fukui, A. Klümper, and C. Scheeren, *J. Phys. Soc. Jpn.* **74**, 181 (2005).
- [15] F. Heidrich-Meisner, A. Honecker, D. C. Cabra, and W. Brenig, *Phys. Rev. B* **68**, 134436 (2003).
- [16] J. Herbrych, P. Prelovšek, and X. Zotos, *Phys. Rev. B* **84**, 155125 (2011).
- [17] C. Karrasch, J. H. Bardarson, and J. E. Moore, *Phys. Rev. Lett.* **108**, 227206 (2012).
- [18] R. Steinigeweg, J. Gemmer, and W. Brenig, *Phys. Rev. Lett.* **112**, 120601 (2014).

- [19] R. Steinigeweg, J. Gemmer, and W. Brenig, *Phys. Rev. B* **91**, 104404 (2015).
- [20] M. Žnidarič, *Phys. Rev. Lett.* **106**, 220601 (2011).
- [21] R. Steinigeweg and W. Brenig, *Phys. Rev. Lett.* **107**, 250602 (2011).
- [22] R. Steinigeweg, F. Jin, D. Schmidtke, H. De Raedt, K. Michielsen, and J. Gemmer, *Phys. Rev. B* **95**, 035155 (2017).
- [23] S. Kirchner, H. G. Evertz, and W. Hanke, *Phys. Rev. B* **59**, 1825 (1999).
- [24] S. Fujimoto and N. Kawakami, *J. Phys. A: Math. Gen.* **31**, 465 (1997).
- [25] N. M. R. Peres, R. G. Dias, P. D. Sacramento, and J. M. P. Carmelo, *Phys. Rev. B* **61**, 5169 (2000).
- [26] J. M. P. Carmelo, S.-J. Gu, and P. Sacramento, *Ann. Phys.* **339**, 484 (2013).
- [27] P. Prelovšek, S. E. Shawish, X. Zotos, and M. Long, *Phys. Rev. B* **70**, 205129 (2004).
- [28] C. Karrasch, D. M. Kennes, and J. E. Moore, *Phys. Rev. B* **90**, 155104 (2014).
- [29] F. Jin, R. Steinigeweg, F. Heidrich-Meisner, K. Michielsen, and H. De Raedt, *Phys. Rev. B* **92**, 205103 (2015).
- [30] C. Karrasch, T. Prosen, and F. Heidrich-Meisner, *Phys. Rev. B* **95**, 060406(R) (2017).
- [31] T. Prosen and M. Žnidarič, *Phys. Rev. B* **86**, 125118 (2012).
- [32] T. Prosen, *Phys. Rev. E* **89**, 012142 (2014).
- [33] J. Gemmer and G. Mahler, *Eur. Phys. J. B* **31**, 249 (2003).
- [34] S. Goldstein, J. L. Lebowitz, R. Tumulka, and N. Zanghi, *Phys. Rev. Lett.* **96**, 050403 (2006).
- [35] S. Popescu, A. J. Short, and A. Winter, *Nat. Phys.* **2**, 754 (2006).
- [36] P. Reimann, *Phys. Rev. Lett.* **99**, 160404 (2007).
- [37] C. Bartsch and J. Gemmer, *Phys. Rev. Lett.* **102**, 110403 (2009).
- [38] C. Bartsch and J. Gemmer, *Europhys. Lett.* **96**, 60008 (2011).
- [39] S. Sugiura and A. Shimizu, *Phys. Rev. Lett.* **108**, 240401 (2012).
- [40] S. Sugiura and A. Shimizu, *Phys. Rev. Lett.* **111**, 010401 (2013).
- [41] T. A. Elsayed and B. V. Fine, *Phys. Rev. Lett.* **110**, 070404 (2013).
- [42] A. Hams and H. De Raedt, *Phys. Rev. E* **62**, 4365 (2000).
- [43] T. Iitaka and T. Ebisuzaki, *Phys. Rev. Lett.* **90**, 047203 (2003).
- [44] T. Iitaka and T. Ebisuzaki, *Phys. Rev. E* **69**, 057701 (2004).
- [45] S. R. White, *Phys. Rev. Lett.* **102**, 190601 (2009).
- [46] T. Monnai and A. Sugita, *J. Phys. Soc. Jpn.* **83**, 094001 (2014).
- [47] See Supplemental Material at <http://link.aps.org/supplemental/10.1103/PhysRevE.96.020105> for additional information on typicality, finite-size scaling, the role of the particle sector, and energy flow.
- [48] R. Steinigeweg, H. Wichterich, and J. Gemmer, *Europhys. Lett.* **88**, 10004 (2009).
- [49] R. Steinigeweg, F. Heidrich-Meisner, J. Gemmer, K. Michielsen, and H. De Raedt, *Phys. Rev. B* **90**, 094417 (2014).
- [50] A. Weiße, G. Wellein, A. Alvermann, and H. Fehske, *Rev. Mod. Phys.* **78**, 275 (2006).
- [51] M. Stephan and J. Docter, *J. Large-Scale Res. Facil.* **1**, A1 (2015).